Acta Crystallographica Section F
Structural Biology and Crystallization Communications
ISSN 1744-3091

Crystallization of *Saccharomyces cerevisiae* aminopeptidase 1, the major cargo protein of the Cvt pathway

Wakana Adachi,[a] Nobuo N. Suzuki,[a] Yuko Fujioka,[a] Kuninori Suzuki,[b] Yoshinori Ohsumi[b] and Fuyuhiko Inagaki[a]*

[a]Department of Structural Biology, Graduate School of Pharmaceutical Sciences, Hokkaido University, N-12, W-6, Kita-ku, Sapporo 060-0812, Japan, and [b]Division of Molecular Cell Biology, National Institute for Basic Biology, 38 Nishigonaka, Myodaiji, Okazaki 444-8585, Japan

Correspondence e-mail: finagaki@pharm.hokudai.ac.jp

Received 7 November 2006
Accepted 1 February 2007

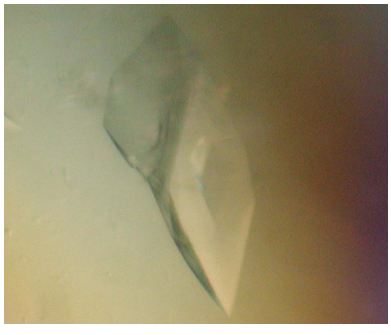

The vacuole hydrolase aminopeptidase 1 (Ape1) is a cargo protein transported to the vacuole by the cytosol-to-vacuole targeting (Cvt) pathway during conditions of growth and by autophagy during conditions of starvation. After transport to the vacuole, Ape1 is processed into mature Ape1 (mApe1). mApe1 has been expressed, purified and crystallized in two crystal forms. Form I belongs to space group $P2_1$, with unit-cell parameters a = 120.6, b = 219.5, c = 133.1 Å, β = 116.5°. Form II belongs to space group $R3$, with unit-cell parameters a = 141.2, c = 349.4 Å. Diffraction data were collected from these crystals to a resolution of 2.5 Å for form I and 1.83 Å for form II. Self-rotation functions and the volume-to-weight ratio values suggest that forms I and II contain 12 and four mApe1 molecules per asymmetric unit, respectively, and that mApe1 exists as a tetrahedral dodecamer in both crystal forms.

1. Introduction

In the yeast *Saccharomyces cerevisiae*, most vacuolar enzymes are transported to the vacuole through the secretory pathway. However, aminopeptidase 1 (Ape1), one of the vacuolar hydrolases, is known to be transported to the vacuole by the cytosol-to-vacuole targeting (Cvt) pathway under growth conditions (Baba *et al.*, 1997; Scott *et al.*, 1997). The Cvt pathway overlaps mechanistically and genetically with autophagy, the bulk degradation process that transports proteins and organelles to the vacuole for degradation. Upon starvation, the Cvt pathway is inhibited, so that Ape1 is exclusively transported to the vacuole by starvation-induced autophagy (Baba *et al.*, 1997; Scott *et al.*, 1997). Ape1 is synthesized in a precursor form (prApe1) that has an amino-terminal propeptide (Oda *et al.*, 1996). Immediately after its synthesis, prApe1 assembles into a multimer, possibly a dodecamer (Kim *et al.*, 1997), and prApe1 multimers subsequently aggregate into a huge complex (the Ape1 complex). The Ape1 complex is then recognized by its receptor, Atg19 (Scott *et al.*, 2001), and Atg19 further interacts with Atg11, which tethers the Ape1–Atg19 complex to the pre-autophagosomal structure (PAS; Yorimitsu & Klionsky, 2005). PAS is the perivacuolar vesicle-forming site where the cargo–receptor complex is selectively enwrapped by a double-membrane structure termed the Cvt vesicle under growth conditions and by a similar but larger double-membrane structure termed the autophagosome under starvation conditions (Suzuki *et al.*, 2001, 2002; Kim *et al.*, 2002). The outer membrane of the Cvt vesicle or the autophagosome then fuses with the vacuole. Together with its component of the Ape1 complex, the inner membrane of the Cvt vesicle/autophagosome is released into the vacuolar lumen. The propeptide of prApe1 is subsequently removed in a proteinase B-dependent reaction to generate mature Ape1 (mApe1; Klionsky *et al.*, 1992). The Ape1 complex is disaggregated in the vacuolar lumen, but mApe1 retains its dodecameric form (Kim *et al.*, 1997; Metz *et al.*, 1977; Loffler & Rohm, 1979) and functions as an aminopeptidase.

The induction of the Cvt pathway (but not the autophagic response) depends on the presence of Ape1 (Shintani & Klionsky, 2004). Therefore, structural studies on Ape1 would be helpful to understand the mechanism of Cvt vesicle formation. In this report, we describe the expression, purification and crystallization of mApe1. Self-rotation functions and the volume-to-weight ratio values of

Table 1
Data-collection statistics.

Values in parentheses are for the highest resolution shell.

Crystal form	I	II
Space group	$P2_1$	$R3$
Resolution range (Å)	50–2.5 (2.59–2.50)	100–1.83 (1.90–1.83)
Wavelength (Å)	1.000	0.800
Observed reflections	680702	995133
Unique reflections	209870	227735
Completeness (%)	98.7 (99.7)	99.9 (100)
$R_{\rm merge}(I)$† (%)	4.8 (33.8)	8.2 (30.5)
$I/\sigma(I)$	27.7 (3.1)	27.1 (4.3)

† $R_{\rm merge}(I) = \left(\sum\sum|I_i - \langle I\rangle|\right)/\sum\sum I_i$, where I_i is the intensity of the ith observation and $\langle I\rangle$ is the mean intensity.

mApe1 crystals suggest that mApe1 exists as a tetrahedral dodecamer in the crystals.

2. Expression and purification

Although full-length Ape1 (prApe1; 514 residues) could be expressed solubly in *Escherichia coli* as a fusion protein with glutathione *S*-transferase (GST), it became insoluble upon removal of the GST. Therefore, mApe1 (residues 46–514; molecular weight 51 691 Da) and Ape1 propeptide (residues 1–45; molecular weight 5418 Da) were separately expressed as follows. Using the *Nco*I–*Sal*I restriction sites, the region encoding residues 46–514 of Ape1 (mApe1) was inserted into a pGEX-6p vector (GE Healthcare Biosciences) which has an *Nco*I site introduced upstream of the *Bam*HI site and a His_6 tag downstream of *Sal*I. Using the *Nde*I–*Bam*HI restriction sites, the region encoding residues 1–45 of Ape1 (Ape1 propeptide) was inserted into a pGEX6p vector which has an *Nde*I site introduced upstream of the *Bam*HI site. mApe1 and Ape1 propeptide were expressed in *E. coli* BL21(DE3) with GST fused at their N-termini. Cells were cultured to an A_{600} of 0.7 at 310 K and induced with 0.1 m*M* isopropyl β-D-thiogalactopyranoside at 293 K for 21 h. After cell lysis, the proteins were first purified by affinity chromatography using a glutathione Sepharose 4B column (GE Healthcare Biosciences) and GST was then cleaved with PreScission protease (GE Healthcare Biosciences). Gly-Pro-Met and Gly-Pro-His sequences remained at the N-terminus of mApe1 and Ape1 propeptide, respectively. mApe1 was then purified by size-exclusion chromatography using a Superdex 200 column (GE Healthcare Biosciences) and was eluted with 20 m*M* Tris buffer pH 8.0 and 150 m*M* NaCl. Purified mApe1 was concentrated to 5 mg ml^{-1} in 150 m*M* NaCl, 20 m*M* Tris–HCl pH 8.0 and 5 m*M* DTT. Ape1 propeptide was initially purified by size-exclusion chromatography using a Superdex 75 column (GE Healthcare Biosciences) eluted with 20 m*M* Tris buffer pH 8.0 and 150 m*M* NaCl. It was further purified by reverse-phase chromatography using a Resource RPC column (GE Healthcare Biosciences) and was concentrated to 4 mg ml^{-1} in 150 m*M* NaCl, 20 m*M* Tris–HCl pH 8.0 and 5 m*M* DTT.

3. Crystallization

Crystallization trials were performed using the sitting-drop vapour-diffusion method with mApe1 alone or a mixture of mApe1 and Ape1 propeptide. Initial screening was performed using Crystal Screen and Crystal Screen II from Hampton Research and Wizard I, Wizard II, Cryo I and Cryo II from Emerald Biostructures. Crystals of mApe1 were obtained in two forms, I and II, from the same reservoir solution consisting of 0.1 *M* Tris–HCl pH 6.5, 30% polyethylene glycol 400, 0.1 *M* $MgCl_2$ and 1.1 *M* NaCl. Form I crystals were obtained by mixing 1.0 µl 5 mg ml^{-1} mApe1 in 150 m*M* NaCl, 20 m*M* Tris–HCl pH 8.0 and 5 m*M* DTT with 1.0 µl reservoir solution and equilibrating against 100 µl reservoir solution at 293 K. The crystals grew to average dimensions of 200 × 200 × 500 µm after 3 d (Fig. 1*a*). Form II crystals were obtained by mixing 2.0 µl 2.5 mg ml^{-1} mApe1, 2.0 mg ml^{-1} Ape1 propeptide in 150 m*M* NaCl, 20 m*M* Tris–HCl pH 8.0 and 5 m*M* DTT with 1.0 µl reservoir solution and equilibrating against 100 µl reservoir solution at 293 K. Form II crystals were observed after two weeks and grew to maximum dimensions of 300 × 300 × 500 µm within two months (Fig. 1*b*). Although form II crystals were obtained from the mixture of mApe1 and Ape1 propeptide, SDS–PAGE analysis showed that they contained only mApe1 (data not shown).

4. Preliminary crystallographic analysis

As mApe1 is a zinc-binding enzyme, the form II crystals (but not the form I crystals) were soaked in reservoir solution supplemented with 1 m*M* zinc acetate instead of 0.1 *M* $MgCl_2$ for 2 h prior to data collection in order to clarify the zinc-chelated structure of the enzyme. The crystals were already cryoprotected by the mother

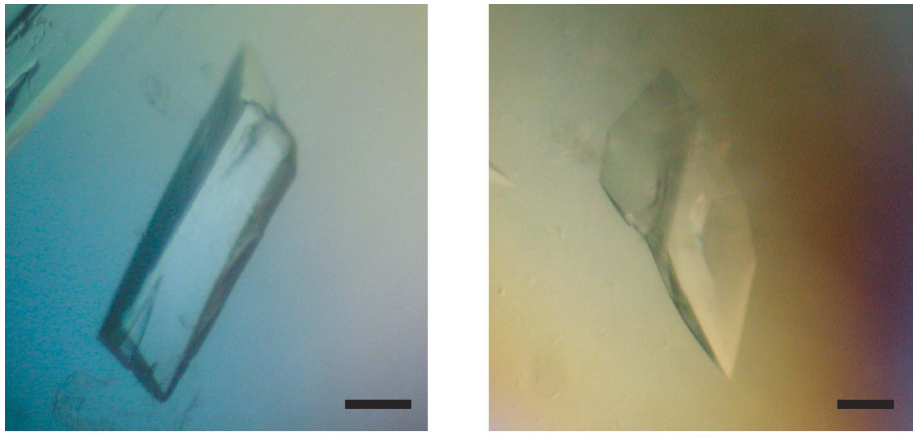

(*a*) (*b*)

Figure 1
Crystals of mApe1. The black scale bar is 100 µm in length.

liquor, so they were flash-cooled directly and kept in a stream of nitrogen gas at 100 K. All diffraction data were collected on an ADSC Quantum 210 charge-coupled device detector at beamline NW12A, KEK, Japan. Diffraction data were indexed, integrated and scaled with the program *HKL*-2000 (Otwinowski & Minor, 1997). The data-collection statistics are summarized in Table 1.

5. Discussion

Form I crystals belong to the monoclinic space group $P2_1$, with unit-cell parameters a = 120.6, b = 219.5, c = 133.1 Å, β = 116.5°. The acceptable range of the volume-to-weight ratio (V_M) value (Matthews, 1968) indicates that form I contains 8–16 protein molecules per asymmetric unit (V_M = 1.9–3.8 Å^3 Da^{-1}). Form II crystals belong to the rhombohedral space group $R3$, with unit-cell parameters a = 141.2, c = 349.4 Å. The V_M values indicate that the form II crystal contains 4–6 protein molecules per asymmetric unit (V_M = 2.2–3.2 Å^3 Da^{-1}). Self-rotation functions were calculated using diffraction data from both crystals. Two sections at κ = 120 and 180° for both forms I and II are shown in Fig. 2. The form II crystal contains four threefold axes, one of which corresponds to a crystallographic axis and the other three of which correspond to noncrystallographic axes. Furthermore, the form II crystal contains three noncrystallographic twofold axes. Since four threefold and three twofold axes are a feature of dodecameric tetrahedral aminopeptidases (Russo & Baumann, 2004; Franzetti *et al.*, 2002), mApe1 in form II crystals also seems to exist as a tetrahedral dodecamer in which one threefold axis of the tetrahedron corresponds to the crystallographic threefold axis. mApe1 was eluted from the size-exclusion column with a retention volume of beyond 400 kDa, but we could not determine the molecular weight more precisely by this method. We also performed analytical ultracentrifugation, but again could not determine the molecular weight of mApe1 precisely because mApe1 showed a propensity towards aggregation. Metz *et al.* (1977) and Loffler & Rohm (1979) report that mApeI exists in the vacuole as a dodecamer

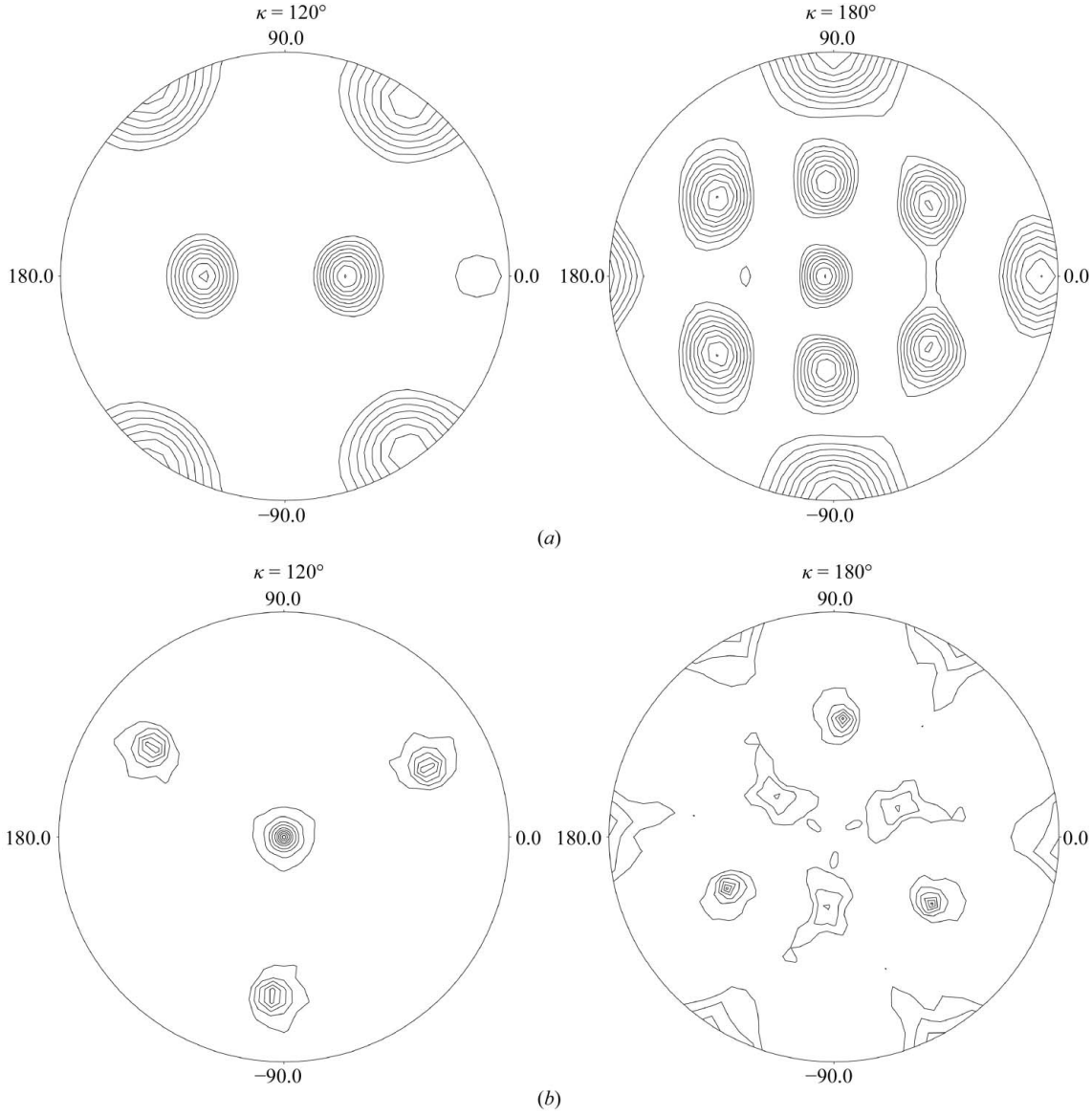

Figure 2
Stereographic projections of the self-rotation functions from the data sets of mApe1 crystals. (*a*) The self-rotation functions of form I data were calculated using a 30 Å radius of integration and data in the resolution range 15–4 Å. (*b*) The self-rotation functions of form II data were calculated using a 45 Å radius of integration and data in the resolution range 15–4 Å.

of identical subunits. Furthermore, Franzetti *et al.* (2002) showed by electron microscopy that TET, an aminopeptidase from archaea, has a dodecameric tetrahedral structure. From these reports, we believe that mApe1 exists as a dodecamer in solution. Thus, form II probably contains four mApe1 molecules per asymmetric unit (V_M = 3.2 Å^3 Da^{-1}, solvent content 62.0%). In contrast, form I contains four noncrystallographic threefold axes and eight noncrystallographic twofold axes. Two tetrahedral dodecamers related by a crystallographic twofold axis could show such a set of noncrystallographic symmetry axes. Thus, in form I crystals mApe1 also seems to exist as a tetrahedral dodecamer and there is a high probability that 12 mApe1 molecules are contained in the asymmetric unit (V_M = 2.5 Å^3 Da^{-1}, solvent content 51.6%). Molecular replacement was performed using the program *MOLREP* (Vagin & Teplyakov, 1997) from the *CCP*4 software suite (Collaborative Computational Project, Number 4, 1994) for the form II data. The crystal structure of aminopeptidase I from *Borrelia burgdorferi* B31 (PDB code 1y7e) was used as the search model. Four molecules were found in the asymmetric unit, which gave us phases that were good enough to calculate an interpretable electron-density map. Crystallographic refinement is now in progress.

We thank the staff at beamline NW12, KEK, Japan for data-collection support. This work was supported by a Grant-in-Aid for Scientific Research on Priority Areas and by the National Project on Protein Structural and Functional Analyses from the Ministry of Education, Culture, Sports, Science and Technology (MEXT), Japan. This work was carried out under the NIBB Cooperative Research Program (4-148).

References

Baba, M., Osumi, M., Scott, S. V., Klionsky, D. J. & Ohsumi, Y. (1997). *J. Cell Biol.* **139**, 1687–1695.
Collaborative Computational Project, Number 4 (1994). *Acta Cryst.* D**50**, 760–763.
Franzetti, B., Schoehn, G., Hernandez, J. F., Jaquinod, M., Ruigrok, R. W. & Zaccai, G. (2002). *EMBO J.* **21**, 2132–2138.
Kim, J., Huang, W. P., Stromhaug, P. E. & Klionsky, D. J. (2002). *J. Biol. Chem.* **277**, 763–773.
Kim, J., Scott, S. V., Oda, M. N. & Klionsky, D. J. (1997). *J. Cell Biol.* **137**, 609–618.
Klionsky, D. J., Cueva, R. & Yaver, D. S. (1992). *J. Cell Biol.* **119**, 287–299.
Loffler, H. G. & Rohm, K. H. (1979). *Z. Naturforsch. C*, **34**, 381–386.
Matthews, B. W. (1968). *J. Mol. Biol.* **33**, 491–497.
Metz, G., Marx, R. & Rohm, K. H. (1977). *Z. Naturforsch. C*, **32**, 929–937.
Oda, M. N., Scott, S. V., Hefner-Gravink, A., Caffarelli, A. D. & Klionsky, D. J. (1996). *J. Cell Biol.* **132**, 999–1010.
Otwinowski, Z. & Minor, W. (1997). *Methods Enzymol.* **276**, 307–326.
Russo, S. & Baumann, U. (2004). *J. Biol. Chem.* **279**, 51275–51281.
Scott, S. V., Baba, M., Ohsumi, Y. & Klionsky, D. J. (1997). *J. Cell Biol.* **138**, 37–44.
Scott, S. V., Guan, J., Hutchins, M. U., Kim, J. & Klionsky, D. J. (2001). *Mol. Cell*, **7**, 1131–1141.
Shintani, T. & Klionsky, D. J. (2004). *J. Biol. Chem.* **279**, 29889–29894.
Suzuki, K., Kamada, Y. & Ohsumi, Y. (2002). *Dev. Cell*, **3**, 815–824.
Suzuki, K., Kirisako, T., Kamada, Y., Mizushima, N., Noda, T. & Ohsumi, Y. (2001). *EMBO J.* **20**, 5971–5981.
Vagin, A. & Teplyakov, A. (1997). *J. Appl. Cryst.* **30**, 1022–1025.
Yorimitsu, T. & Klionsky, D. J. (2005). *Mol. Biol. Cell*, **16**, 1593–1605.